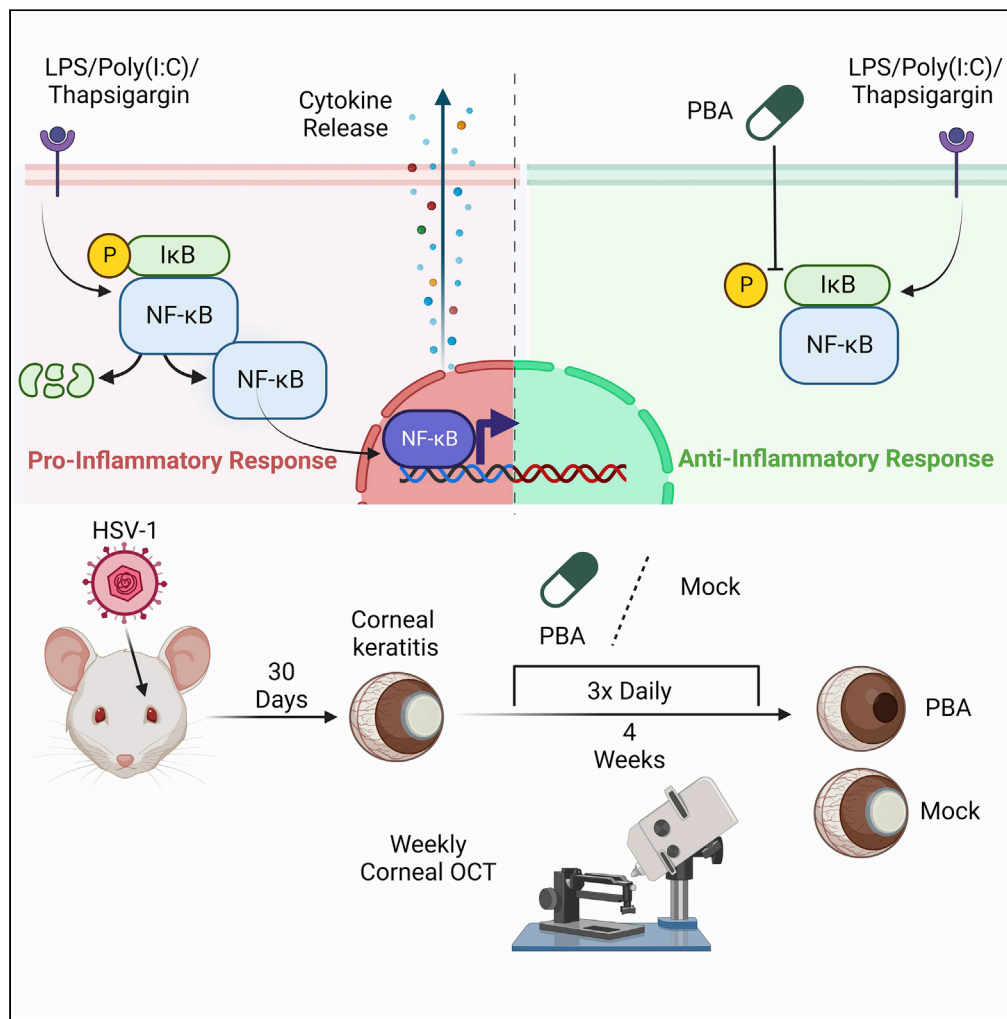


Article

Topical phenylbutyrate antagonizes NF- κ B signaling and resolves corneal inflammation



Raghuram Koganti, Tejabhiram Yadavalli, Yogesh Sutar, Sudipta Mallick, Abhijit Date, Deepak Shukla

dshukla@uic.edu

Highlights
PBA inhibits inflammation in preclinical ocular-inflammation models

PBA prevents the production of pro-inflammatory cytokines by inhibiting NF- κ B

PBA quickens the resolution of herpetic keratitis in mice

PBA synergizes with the corticosteroid dexamethasone to antagonize NF- κ B signaling

Koganti et al., iScience 25, 105682
December 22, 2022 © 2022 The Authors.
<https://doi.org/10.1016/j.isci.2022.105682>



Article

Topical phenylbutyrate antagonizes NF- κ B signaling and resolves corneal inflammation

Raghuram Koganti,^{1,5} Tejabhiram Yadavalli,^{1,5} Yogesh Sutar,^{2,3} Sudipta Mallick,² Abhijit Date,^{2,3} and Deepak Shukla^{1,4,6,*}

SUMMARY

Chronic inflammation of the immune privileged cornea originating from viral or nonviral conditions results in significant vision loss. Topical corticosteroids are the common treatments for corneal inflammation, but the drugs cause serious and potentially blinding side effects in the long term. Therefore, new standalone and/or synergistic anti-inflammatory therapies with lower side effects are desperately needed. Here, we show that the aromatic fatty acid phenylbutyrate (PBA) acts as a potent inhibitor of inflammation in preclinical ocular-inflammation models. PBA prevents the transcription as well as translation of pro-inflammatory cytokines by LPS and poly(I:C) via persistent inhibition of NF- κ B signaling. PBA quickens the resolution of ocular inflammation in mice by decreasing corneal thickness and immune cell infiltration. More importantly, PBA can synergize with the dexamethasone to antagonize NF- κ B signaling at lower drug concentrations. Our results demonstrate that PBA therapy exerts previously unreported anti-inflammatory effects in the eye and facilitates corneal healing during persistent inflammation.

INTRODUCTION

Recurrent and/or persistent inflammation of the eye due to viral or nonviral diseases is a leading cause of ocular pain and blindness. Ocular inflammatory diseases and disorders constitute the major class of conditions that cause blindness.¹ Among viral causes, herpes simplex virus 1 (HSV-1) infection of the eye and its recurrent episodes are known to be the leading cause of persistent inflammation resulting in permanent clouding of the cornea. Herpetic keratitis and uveitis both persist for long duration and turn into a source of continuous pain and discomfort in the eye. Persistent inflammation is the main reason why HSV-1 is considered the most common cause of infection-associated blindness in the developed world.² Treatment requires long-term use of topical corticosteroids, which itself can give rise to cataract formation or even more serious and potentially blinding, glaucoma, in many cases.³ Thus, the ocular side effects originating from the long-term use of commonly prescribed corticosteroids require development of more specific and safer drugs to treat ocular inflammatory diseases. 4-phenylbutyrate (PBA) is an aromatic, short-chain fatty acid which has been reported to play a variety of roles in the body. It is well known as an FDA-approved ammonia scavenger for the treatment of urea cycle disorders.⁴ However, PBA also acts as a chemical chaperone to relieve ER stress^{5,6} and as a pan-histone deacetylase (HDAC) inhibitor which may suppress proliferation of specific types of cancers.^{7,8} Recently, PBA has been shown to inhibit inflammation in models of neuronal or lung injury, primarily through the alleviation of ER stress and the subsequent inflammatory response.^{9–13} PBA has been shown to reduce ocular hypertension in murine models of glaucoma,^{14–16} but its anti-inflammatory effects in preclinical models of ocular inflammation have not been well elucidated.

PBA can exert antiviral activity against HSV-1 and HSV-2 when administered systemically through intraperitoneal injections.¹⁷ While systemically administered NaPBA strongly indicated that PBA could be repurposed for the treatment of HSV-1 infection, topical administration of PBA or NaPBA, for reasons unknown, did not show antiviral efficacy in ocular models of HSV infection.¹⁷ It is likely that topical PBA is inefficient due to inadequate penetration, retention, and delivery of the drug through the mucus barrier of the corneal epithelium resulting in the sub-therapeutic concentrations in the ocular tissue and therefore, less effective in reducing HSV-1 infection via topical applications.

¹Department of Ophthalmology and Visual Sciences, University of Illinois Medical Center, 1855 W. Taylor Street, MC 648, Chicago, IL 60612, USA

²Department of Pharmaceutical Sciences, The Daniel K. Inouye College of Pharmacy, University of Hawaii Hilo, Hilo, HI 96720, USA

³R. Ken Coit College of Pharmacy, The University of Arizona, Tuscon, AZ 85721, USA

⁴Department of Microbiology and Immunology, University of Illinois at Chicago, Chicago, IL 60612, USA

⁵These authors contributed equally

⁶Lead contact

*Correspondence: dshukla@uic.edu

<https://doi.org/10.1016/j.isci.2022.105682>



The presence of mucin layer in the tear-film poses a significant barrier for the ocular delivery of various drugs. The mucin layer, due to its complex mesh-like structure, can trap foreign molecules including drugs and particles due to adhesive interactions; thus, preventing effective delivery to the corneal epithelium. Poloxamer 407 is an FDA-approved amphiphilic polymeric surfactant approved for oral, parenteral, and topical (vaginal, dermal, and ocular routes).^{18–21} Poloxamer 407 is commonly used in various ocular formulations. Interestingly, Poloxamer 407-coated nanoparticles (NPs) of size ~200 nm have shown the capability to penetrate through the mucin layer present at various mucosal surfaces including the eye.^{22,23} Moreover, this mucus-penetrating strategy has culminated in the translation and FDA approval of two eye drop products (EYsuVIS and INVELTYS) containing Poloxamer 407-coated loteprednol etabonate nanoparticles for the treatment of dry eye symptoms and/or ocular inflammation.^{24,25} The transformation of loteprednol etabonate to mucus-penetrating loteprednol etabonate nanoparticles resulted in a reduction in therapeutic dose as well as dosing frequency which validated the significance of developing mucus-penetrating nanoformulations for topical delivery of drugs.^{26–28}

In this study, we demonstrate that through the use of non-ionic surfactant P407, the antiviral efficacy of topically instilled PBA is improved. We also show that PBA inhibits cytokine induction and release across a diverse set of pro-inflammatory stimuli in human corneal epithelial (HCE) cells and THP-1 macrophages. We demonstrate that PBA can alleviate inflammation through the inhibition of NF- κ B signaling in these models. We confirm these results *in vivo* using a murine model of herpetic keratitis and measuring decreases in corneal thickness and immune cell infiltration with PBA treatment. Finally, we show that PBA can synergize with the currently prescribed corticosteroid dexamethasone to restrict pro-inflammatory signaling.

RESULTS

Topical instillation of P407-loaded PBA effectively reduces viral load

Our loading studies showed that sodium-free P407-PBA-NPs of size ~100 nm can be developed using a simple nanoprecipitation method. We were able to achieve a PBA concentration of 10 mg/mL (~61 mM) in the current formulation. To understand whether these NaPBA-loaded P407 gel retain their antiviral efficacy, we treated cultures of HCE cells infected with HSV-1 strain 17 GFP. The NaPBA gel demonstrated modest antiviral efficacy at the 24 h post infection (hpi) (Figures 1A and 1B). To check whether this topical formulation of NaPBA is physiologically relevant, we tested it on a murine model of ocular HSV-1 infection. Mice were infected in the right eye followed by topical instillation of NaPBA gel 3-times daily for 7 days starting 1 day post infection (dpi). Topical GCV (0.1%) and blank PBS were used as positive and negative controls, respectively. Ocular washes from infected eyes were titrated for the amount of infectious virus on 2 and 4 dpi. While the amount of viral load trended to be on the lower side for NaPBA gel compared to mock on day 2, there was no significant difference in the viral load on days 2 and 4 post infection (Figures 1C and 1D). On the contrary, interestingly, eyes of the animals topically treated with NaPBA gel were pristine and appeared non-infected with no indications of blepharitis, periocular lesions or inflammation, scarring, or visible opacity of the cornea indicating a low disease score (Figures 1E and 1F). Interestingly, Kolliphor P407 alone-treated animals showed lower plaque counts indicating antiviral potential for this gel; however, the periocular inflammation seemed to be greater than NaPBA gel-treated mice (Figures S1A and S1B). All the animals in the NaPBA gel-treated group had non-inflamed eyes that remained that way all until 14 days post infection (Figures S1A–S1C) at which point the experiment was terminated.

PBA alleviates ER stress-induced cytokine production

The results mentioned above are both interesting and confusing given that the antiviral activity did not improve with the topical addition of NaPBA gel. Our previous study showed that PBA topical treatment is not very effective in controlling viral replication in the cornea and now NaPBA delivery through P407 gel only showed limited antiviral efficacy. On the other hand, the pristine eyes without inflammation seen in NaPBA gel-treated animals were very encouraging. As mentioned earlier, previous reports have shown the ability of PBA in reducing ER stress which indirectly helps in the alleviation of inflammation. Based on these results, we hypothesized that PBA through the alleviation of ER stress ameliorates ocular inflammation. To test our hypothesis, we first generated an HCE model of ER stress-induced inflammation to understand whether PBA can alleviate it.

To generate an *in vitro* model of inflammation, we treated HCE cells with the ER stress inducer thapsigargin (TG) for 1 h and measured cytokine transcripts 3 h post treatment (hpt) using qRT-PCR. TG upregulated the expression of the pro-inflammatory cytokines TNF- α , IL-6, and IL-8 in a dose-dependent manner

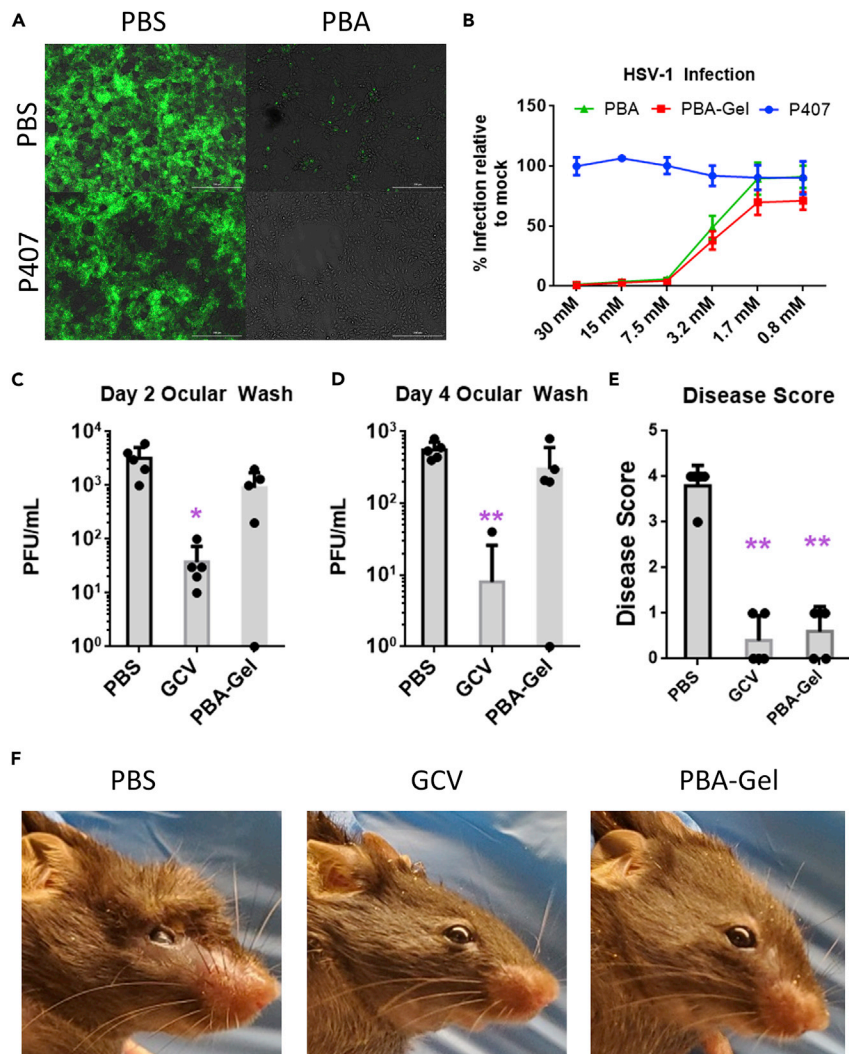


Figure 1. P407-loaded PBA inhibits viral replication and ameliorates induced HSV-1-induced inflammation: HCEs were infected with 17 GFP at 0.1 MOI and treated with PBS, P407, PBA, or PBA-P407 for 24 h

(A) Fluorescent images showing infected cells in green.

(B) Quantification of images in A ($n = 3$). Mice ($n = 5$) were infected with 1×10^5 PFU HSV-1 strain McKrae followed by daily three times dosing of indicated treatments.

(C and D) Ocular washes collected on days 2 and 4 were overlaid on Vero cells to titrate the amount of infectious virus in the animal eyes.

(E) At 7 days post infection, animals were visually examined by a blinded reviewer to score the extent of disease and the scores were plotted.

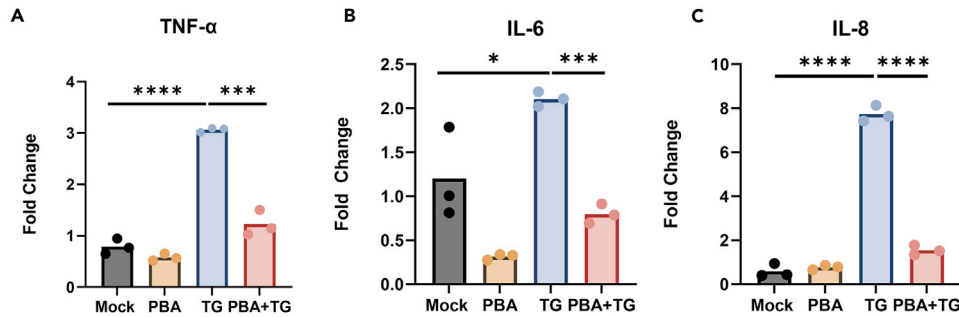
(F) Representative images of periocular region of infected animals treated with shown therapeutics. All data were analyzed using a one-way ANOVA.

* $p < 0.05$; ** $p < 0.01$.

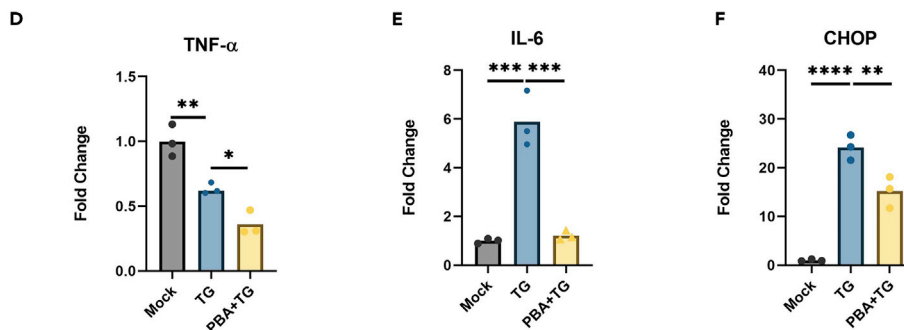
(Figures S2A–S2C). At $10 \mu\text{M}$, TG was found to significantly induce the expression of all three cytokines. We then examined whether PBA could reduce the cytokine upregulation caused by TG. After stimulating the HCE cells with TG, we treated the cells with either 5 mM PBA or DMSO as a control and measured cytokine transcripts 3 hpt. PBA treatment significantly reduced the expression of the pro-inflammatory cytokines TNF- α , IL-6, and IL-8 as compared to DMSO treatment (Figures 2A–2C).

To understand whether this was a cell type-specific phenomenon, we utilized THP-1 cells which are monocyte precursors that can be differentiated into a macrophage-like phenotype. While TG did not stimulate TNF- α expression in THP-1 cells (Figure 2D), it significantly increased the expression of IL-6 and the ER

Human Corneal Cells



Human Monocytes



Multiplex ELISA

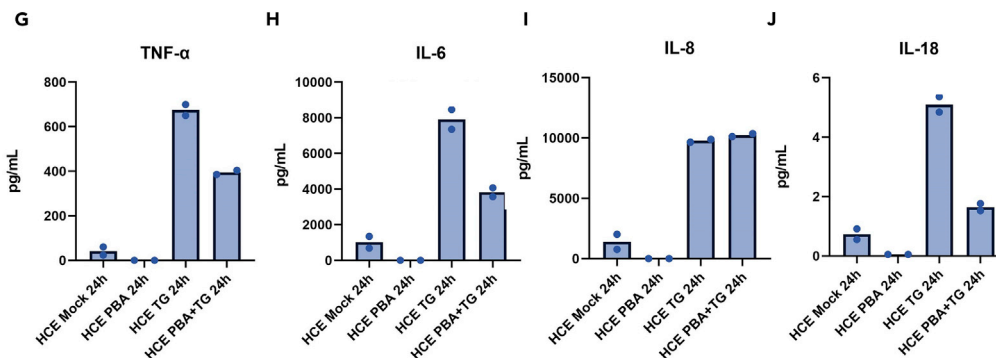


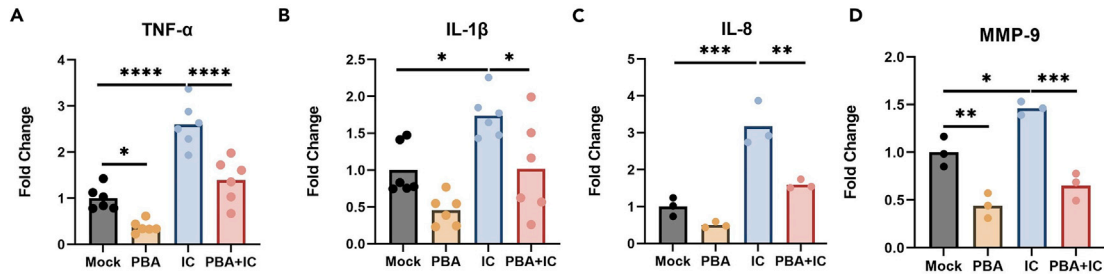
Figure 2. PBA reduces TG-induced cytokine production

Human corneal epithelial (HCE) cells were treated with 10 μ M TG for 1 h or DMSO (mock) before changing the media to either 5 mM PBA or DMSO (control) in MEM. At 4 h post TG treatment, the cells were collected and processed for qRT-PCR. Transcript levels of TNF- α (A), IL-6 (B), and IL-8 (C) were measured ($n \geq 2$). An identical process was utilized for human monocyte (THP-1) cells with the exception of using 20 mM PBA, and the cytokine transcripts of TNF- α (D), IL-6 (E), and CHOP (F) were analyzed ($n = 3$). Representative protein levels of TNF- α (G), IL-6 (H), IL-8 (I), and IL-18 (J) were analyzed using a Multiplex ELISA at 24 h post TG stimulation with PBA or DMSO added afterward as treatments ($n = 2$ in duplicates). All data were analyzed using one-way ANOVA for transcripts and two-way ANOVA for ELISA.

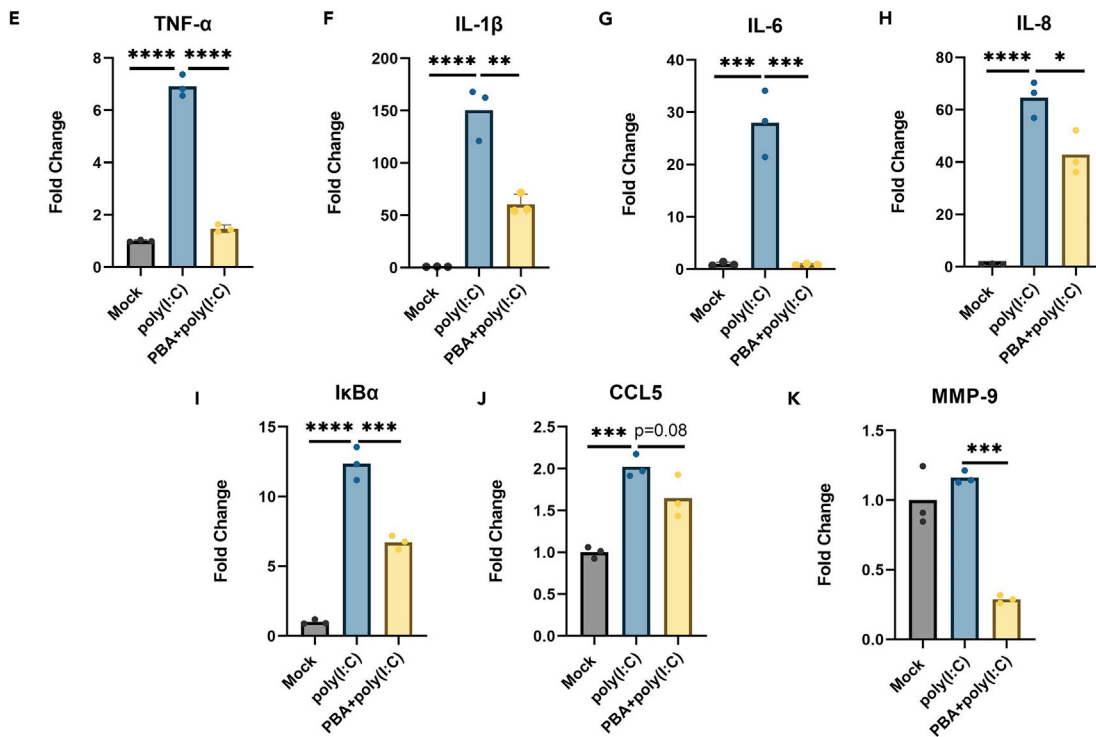
* $p < 0.05$; ** $p < 0.01$; *** $p < 0.001$; and **** $p < 0.0001$.

stress marker CHOP (Figures 2E and 2F). PBA treatment in THP-1 cells significantly reduced the increases in IL-6 and CHOP induced by TG (Figures 2D and 2E). Although the cytokine transcripts increased with TG and decreased with subsequent PBA treatment, we wanted to confirm our findings at the protein level. Using a Multiplex ELISA, we measured a panel of pro-inflammatory cytokines in HCE cells after TG and PBA

Human Corneal cells



Human Monocytes



Multiplex ELISA

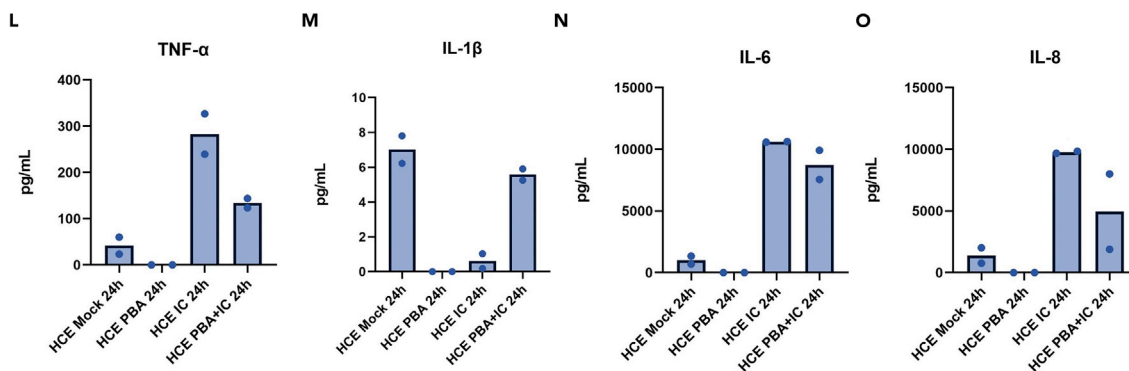


Figure 3. PBA ameliorates poly(I:C)-induced cytokine production

HCE cells were treated with 25 $\mu\text{g}/\text{mL}$ of poly(I:C) for 1 h before changing the media to either 5 mM PBA or DMSO (control) in MEM. At 3 h post poly(I:C) treatment, the cells were collected and processed for qRT-PCR. Transcript levels of TNF- α (A), IL-1 β (B), IL-8 (C), and MMP-9 (D) were measured ($n \geq 3$). An identical process was utilized for human monocyte (THP-1) cells with the exception of using 20 mM PBA, and the cytokine transcripts of TNF- α (E), IL-1 β (F), IL-6 (G), IL-8 (H), I κ B α (I), CCL5 (J), and MMP-9 (K) were analyzed using qRT-PCR ($n = 3$). Representative protein levels of TNF- α (l), IL-1 β (M), IL-6 (N), and IL-8 (O) were analyzed using a Multiplex ELISA at 24 h post poly(I:C) stimulation with PBA or DMSO added afterward as treatments ($n = 2$ in duplicates). All data were analyzed using a one-way ANOVA for transcripts and two-way ANOVA for ELISA.

* $p < 0.05$; ** $p < 0.01$; *** $p < 0.001$; and **** $p < 0.0001$.

treatments using two replicates. We found that TG induced the production of TNF- α , IL-6, IL-8, and IL-18 (Figures 2G–2J). Therapeutic PBA treatment reduced the production of TNF- α , IL-6, and IL-18 proteins, but it was not effective at reducing IL-8 levels.

PBA reduces poly(I:C)-induced cytokine production

As PBA is a known inhibitor of ER stress,⁶ we did not know whether its inhibition of TG-induced inflammation would hold for other types of inflammatory stimulants as well. To test whether PBA could reduce inflammation caused by sources other than ER stress, we stimulated HCE cells with the viral dsRNA mimetic poly(I:C). At 3 hpt, we found that poly(I:C) caused a significant upregulation of multiple pro-inflammatory cytokines in HCE cells (3a–d). Treatment with PBA resulted in a corresponding decrease in cytokine transcripts (Figures 3A–3D). In THP-1 cells, the effects of poly(I:C) were more potent as it induced significant increases in TNF- α , IL-1 β , IL-6, IL-8, I κ B α , and CCL5 transcripts (Figures 3E–3K). PBA treatment after stimulation with poly(I:C) neutered the increase in pro-inflammatory cytokine expression in all the above proteins except CCL5 (Figures 3E–3K). Using the Multiplex ELISA, we observed that poly(I:C) increased TNF- α protein levels in HCE cells while PBA treatment resulted in a corresponding decrease (Figure 3L). Poly(I:C) did not cause an increase in IL-1 β protein secretion (Figure 3M). PBA treatment was insufficient to reduce the cytokine levels of IL-6 and IL-8 post poly(I:C) treatment although there was a trend for a decrease in cytokine production (Figures 3N–3O).

PBA ameliorates LPS-induced cytokine production

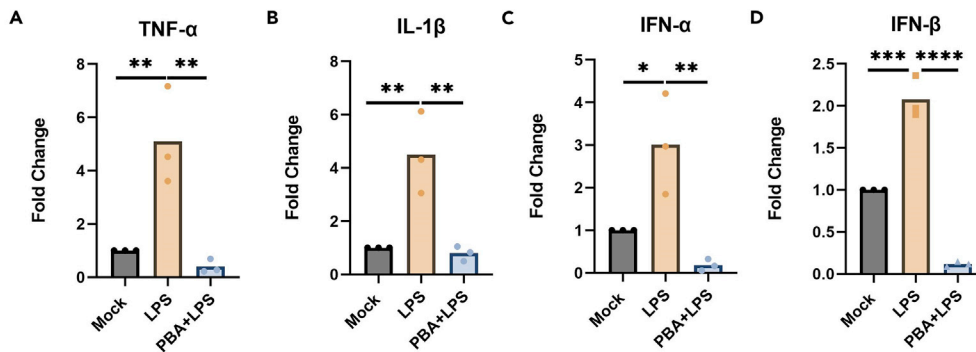
As PBA could reduce cytokine production in HCE and THP-1 cells following stimulation with the viral dsRNA mimetic poly(I:C), we examined whether PBA could reduce inflammation caused by a bacterial source as well. PBA has been shown to reduce TNF- α transcript levels after LPS treatment in murine corneal cells but not human corneal cells.²⁹ Accordingly, we stimulated HCE cells with the bacterial endotoxin lipopolysaccharide (LPS) and found that it significantly increased the expression of TNF- α , IL-1 β , IFN- α , and IFN- β (Figures 4A–4D). As with its efficacy in antagonizing TG and poly(I:C), PBA treatment reduced the cytokine transcripts produced post LPS addition (Figures 4A–4D). Furthermore, PBA abrogated cytokine upregulation in THP-1 cells as seen by declines in TNF- α , IL-1 β , IL-6, IL-8, I κ B α , and CCL5 (Figures 4E–4K). Multiplex ELISA confirmed the qRT-PCR results as PBA treatment inhibited the increases in multiple pro-inflammatory cytokines stimulated by LPS apart from IFN- α which was not stimulated (Figures 4L–4O).

To ensure that these reductions in cytokine expression were specific to PBA as opposed to the addition of a general drug, we treated THP-1 cells with acyclovir (ACV), an inhibitor of HSV replication, post LPS treatment. ACV was insufficient to decrease LPS-induced cytokine expression (Figures S3A–S3F). To better understand the kinetics of LPS-mediated cytokine upregulation, we treated THP-1 cells with either LPS alone or LPS with PBA over multiple time points and observed the levels of cytokine transcripts. Using TNF- α and IL-6 as model endpoints, we observed that PBA blunted transcript increase at all the time points observed while LPS alone caused them to wax and wane over time (Figures S4A and S4B).

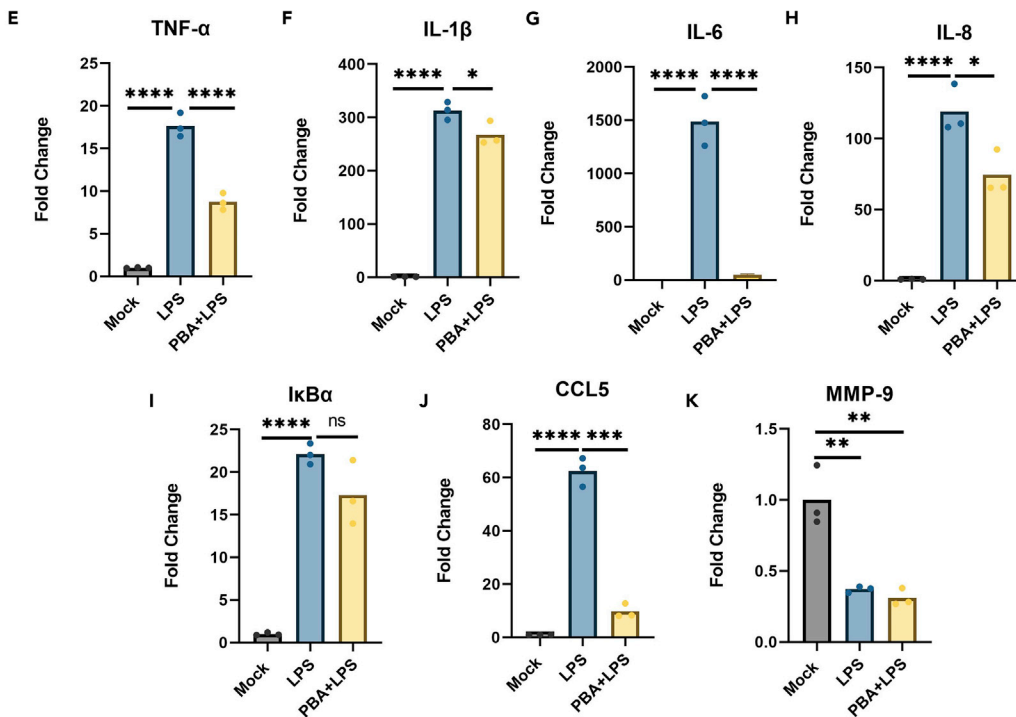
PBA reduces chronic inflammation in mice with herpetic keratitis

Having found that PBA acted as an effective anti-inflammatory *in vitro*, we then investigated whether it could be used as a topical anti-inflammatory therapy as well. We infected mice ($n = 50$) ocularly with HSV-1 and waited four weeks for the infection to clear. 22 of the mice (44%) developed chronic herpetic keratitis as characterized by thickening of the cornea, neovascularization, and ulcer formation. The 22 mice with keratitis were then split into two groups ($n = 11$ per group) and treated three times/day with topical PBA or DMSO formulations. OCT imaging was performed at weekly intervals to assess changes in corneal thickness (Figure 5A). At three and four weeks of topical dosing, the PBA-treated mice displayed significant decreases in corneal thickness compared to their initial state prior to treatment (Figures 5B and

Human Corneal Cells



Human Monocytes



Multiplex ELISA

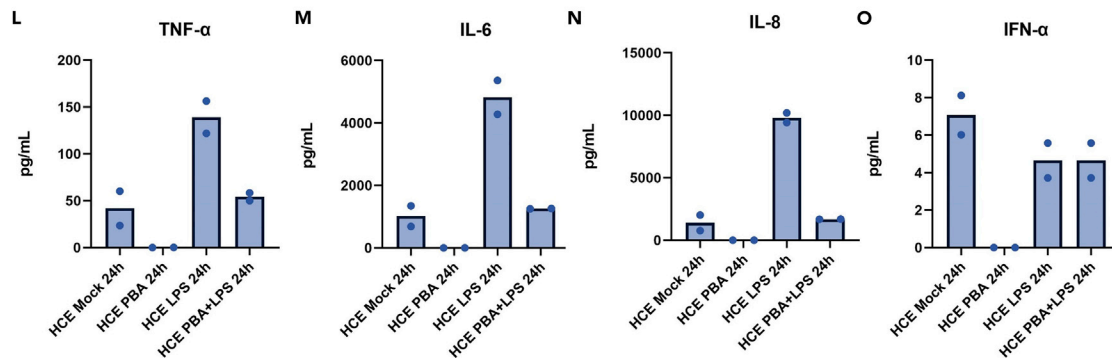


Figure 4. PBA reduces LPS-induced cytokine production

HCE cells were treated with 5 μ g/mL of LPS for 1 h before changing the media to either 5 mM PBA or DMSO (control) in MEM. At 4 h post LPS treatment, the cells were collected and processed for qRT-PCR. Transcript levels of TNF- α (A), IL-1 β (B), IFN- α (C), and IFN- β (D) were measured ($n \geq 3$). An identical process was utilized for human monocyte (THP-1) cells with 100 ng/mL LPS and 20 mM PBA, and the cytokine transcripts of TNF- α (E), IL-1 β (F), IL-6 (G), IL-8 (H), I κ B α (I), CCL5 (J), and MMP-9 (K) were analyzed using qRT-PCR ($n = 3$). Representative protein levels of TNF- α (L), IL-6 (M), IL-8 (N), and IFN- α (O) were analyzed using a Multiplex ELISA at 24 h post LPS stimulation with PBA or DMSO added afterward as treatments ($n = 2$ in duplicates). All data were analyzed using a one-way ANOVA for transcripts and two-way ANOVA for ELISA.

* $p < 0.05$; ** $p < 0.01$; *** $p < 0.001$; and **** $p < 0.0001$.

5C). Corneal opacity was also decreased in the PBA-treated group (Figure 5B). Additionally, PBA treatment was significantly more effective than the DMSO control at treating keratitis 4 weeks post dosing (Figures 5B and 5C). After 4 weeks of dosing and 8 weeks post infection, the animals were euthanized, and their eyes were removed for H&E staining. Representative images of corneal sections of non-infected, infected with DMSO treatment, and infected with PBA treatment are given in Figure S5A. While the DMSO-treated mice showed significant increases in corneal thickness and immune cell infiltration to the deep layers of the cornea, these traits were ameliorated in the PBA-treated group (Figures S5A and S5B).

PBA inhibits NF- κ B-mediated signaling

To identify the mechanism by which PBA blocks inflammation after addition of a variety of stimulants (TG, poly(I:C), and LPS), we examined the effects of PBA on the NF- κ B pathway, a signaling pathway involved in a number of inflammatory responses.^{30,31} The phosphorylation of I κ B α is a well-known marker for NF- κ B activation as it allows for NF- κ B dimers to enter the nucleus and promote transcription of pro-inflammatory cytokines. Western blotting of HCE and THP-1 cells treated with either LPS or poly(I:C) demonstrated that both stimulants increased *p*-I κ B α levels at 4 hpt (Figures 6A and 6B). However, treatment with PBA inhibited the phosphorylation of I κ B α in both cell types and with both stimulants (Figures 6A, 6B, and S6A–S6D).

Degradation of I κ B α classically occurs after its phosphorylation but we did not observe significant degradation with the dosages and cell types present in our models. This may be due in part to the increase in I κ B α transcription and translation after stimulation with LPS or poly(I:C) (Figures 3I and 4I).³² However, we found that treating THP-1 cells with 1 μ g/mL LPS, 10 times higher than our usual dosage, resulted in the degradation of I κ B α after 30 min, and the addition of PBA with LPS reduced the degradation observed (Figure S7). Phosphorylation of NF- κ B p65 is also associated with enhanced transcriptional activity.³³ Similar to the previous findings with *p*-I κ B α , PBA treatment inhibited phosphorylation of p65 in HCE and THP-1 cells after LPS or poly(I:C) stimulation (Figures 6C and 6D, Figures S7E–S7H).

Having observed the potent inhibitory effects of PBA on the phosphorylation of key NF- κ B intermediaries, we next checked whether PBA impeded the nuclear translocation NF- κ B. As NF- κ B dimers translocate to the nucleus following the phosphorylation of *p*-I κ B α , the location of the p65 protein is an established marker for NF- κ B nuclear translocation. Confocal microscopy revealed that nuclear translocation of p65 was increased following LPS treatment in THP-1 cells, but p65 was precluded from the nucleus when PBA was added post LPS stimulation (Figure 6E).

PBA synergizes with the steroid dexamethasone

While PBA proved to be an effective anti-inflammatory agent alone, we wanted to examine whether it could work in synergy with existing, FDA-approved anti-inflammatory medications. To measure whether PBA had any synergistic activity, we stimulated THP-1 cells with LPS and treated them with various concentrations of the steroid dexamethasone (DEX) and PBA. Afterward, the cells were fixed and stained for *p*-I κ B α expression using confocal microscopy. Both PBA and DEX were effective at inhibiting the phosphorylation of I κ B α at higher dosages (Figures 7A and 7B). However, at 5 mM PBA and 6.2 μ M DEX, the combination of drugs displayed a synergistic effect in reducing *p*-I κ B α levels in the THP-1 cells (Figures 7A and 7B). We also found that PBA (1.2 mM) and DEX (6.2 μ M) synergized to inhibit the phosphorylation of p65 as well (Figures 7C and 7D). The PBA/DEX combination achieved comparable efficacy to much greater dosages of each drug individually at reducing *p*-I κ B α and *p*-p65 levels, suggesting that the anti-inflammatory effects of PBA synergized with DEX.

DISCUSSION

Our study demonstrated a previously unreported potent anti-inflammatory activity of PBA against a variety of inflammatory stimulants. Using preclinical models, we found that PBA could restrict expression of

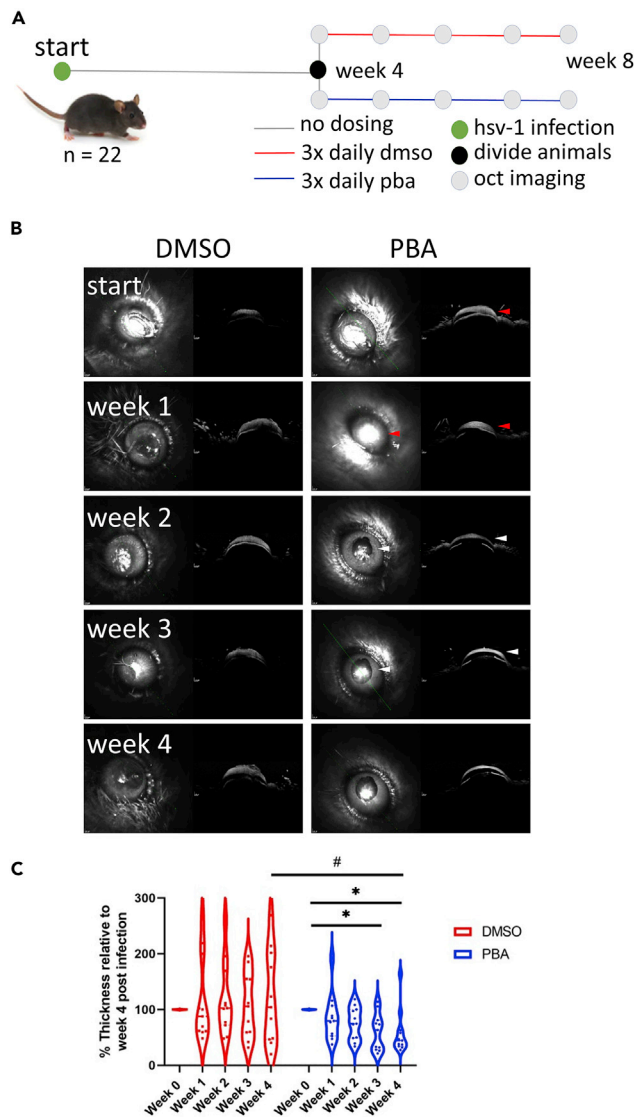


Figure 5. Therapeutic efficacy of PBA for herpes simplex keratitis

6- to 8-week-old C57BL/6 mice ($n = 50$) were infected with 1×10^5 PFU/mL HSV-1 McKrae to the ocular surface after corneal debridement.

Mice were left untreated for 4 weeks post infection to allow for the development of herpetic keratitis. The mice which developed keratitis ($n = 22$) were split into two groups and treated with either 5 mM PBA or DMSO topically three times a day. OCT imaging was performed each week to monitor gross eye pathology and corneal thickness.

(A) Graphic illustrating experimental design.

(B) OCT images of DMSO- or PBA-treated mice with keratitis from weeks 0–4 post treatment. Red arrows on the eye image indicate the opacity of the eye, while red arrows on the OCT image indicate the absence of differentiation between cornea and stroma. White arrows point out the clarity in the ocular image and the differentiation between cornea and sclera in the OCT image.

(C) Quantification of corneal thickness of the two experimental groups using ImageJ.

* $p < 0.05$.

pro-inflammatory cytokines possibly through the inhibition of NF- κ B and facilitate healing of otherwise persistent herpetic keratitis. Inflammation is a necessary physiological response to injury or infection. It promotes the shuttling of blood and leukocytes to the site of injury which minimizes further damage to the affected tissue and promotes healing.³¹ However, excessive or recurrent inflammation can be detrimental and contribute to an array of diseases such as autoimmune disorders, cardiovascular disease, GI disorders, neurodegenerative diseases, and cancer.³¹ Sustained or recurrent inflammation of the cornea, an immune

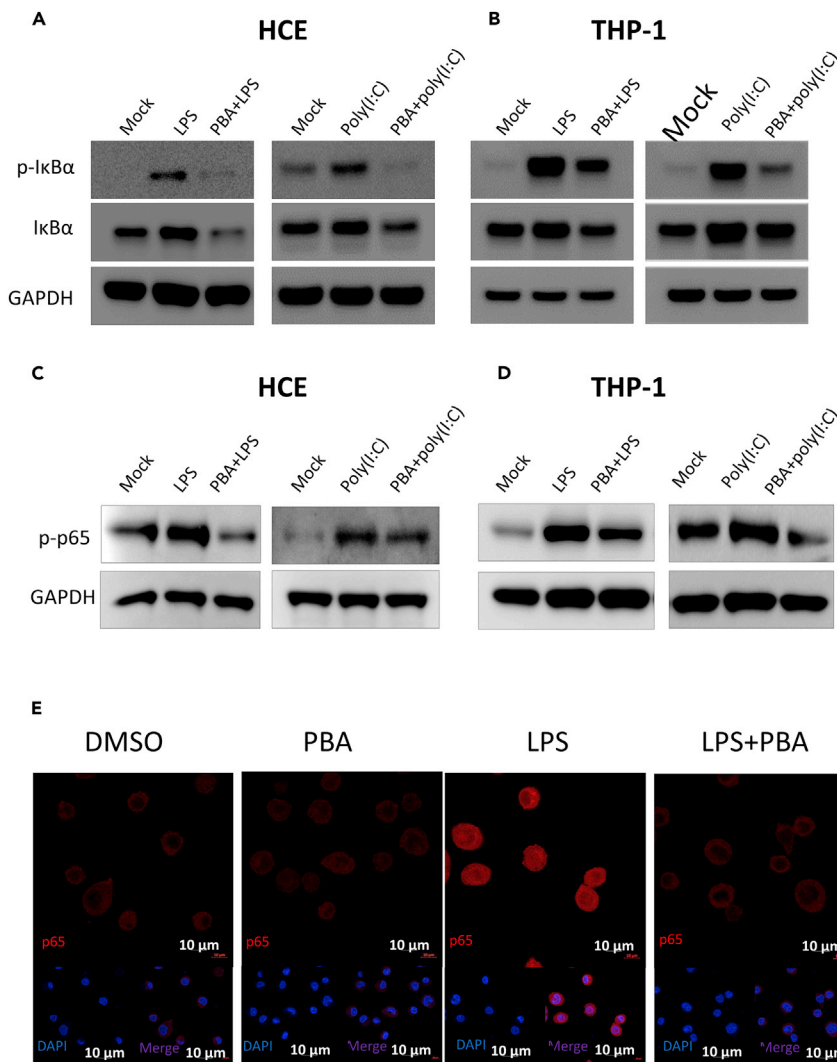


Figure 6. PBA inhibits NF-κB-mediated signaling. HCE and THP-1 cells were stimulated with either LPS or poly(I:C) prior to treatment with PBA (5 mM for HCE cells and 20 mM for THP-1 cells)

At 4 h post treatment, the cells were collected and processed for western blotting. Expression of p-IκBα, IκBα, and GAPDH was measured for both HCE

(A) and THP-1 cells (B). Expression of p-p65 and GAPDH was measured for both HCE (C) and THP-1 cells (D) as well at 2 h post treatment.

(E) PBA inhibits p65 nuclear translocation. THP-1 cells were treated with DMSO, PBA, 1 μg/mL LPS, or LPS + PBA (20 mM) for 15 min. The cells were then fixed, permeabilized, and stained for p65 using immunofluorescence microscopy. Expression of DAPI (blue) and p65 (red) is provided for each sample along with a merged image. Images were taken at 63× magnification.

privileged tissue, is considered a leading cause of vision loss and/or blindness. Likewise, systemic inflammation is a leading cause of disability and mortality in humans.³⁴ Pharmacological aids are often prescribed to curb the inflammatory response and restore homeostasis in the affected tissues. However, current anti-inflammatory medications such as NSAIDs and corticosteroids can lead to severe side effects with chronic usage.³⁵ Thus, there exists a significant demand for additional anti-inflammatory medications to be implemented as alternatives or in conjunction with current therapies.

PBA is currently an FDA-approved drug for the treatment of urea cycle disorders. PBA can be administered orally and is indicated in patients without hepatic or renal insufficiency.³⁶ Less than 2% of patients on PBA therapy report moderate side effects such as renal tubular acidosis or aplastic anemia.³⁶ One therapeutic indication for PBA may be in the treatment of herpetic keratitis. Topical steroid medications such as

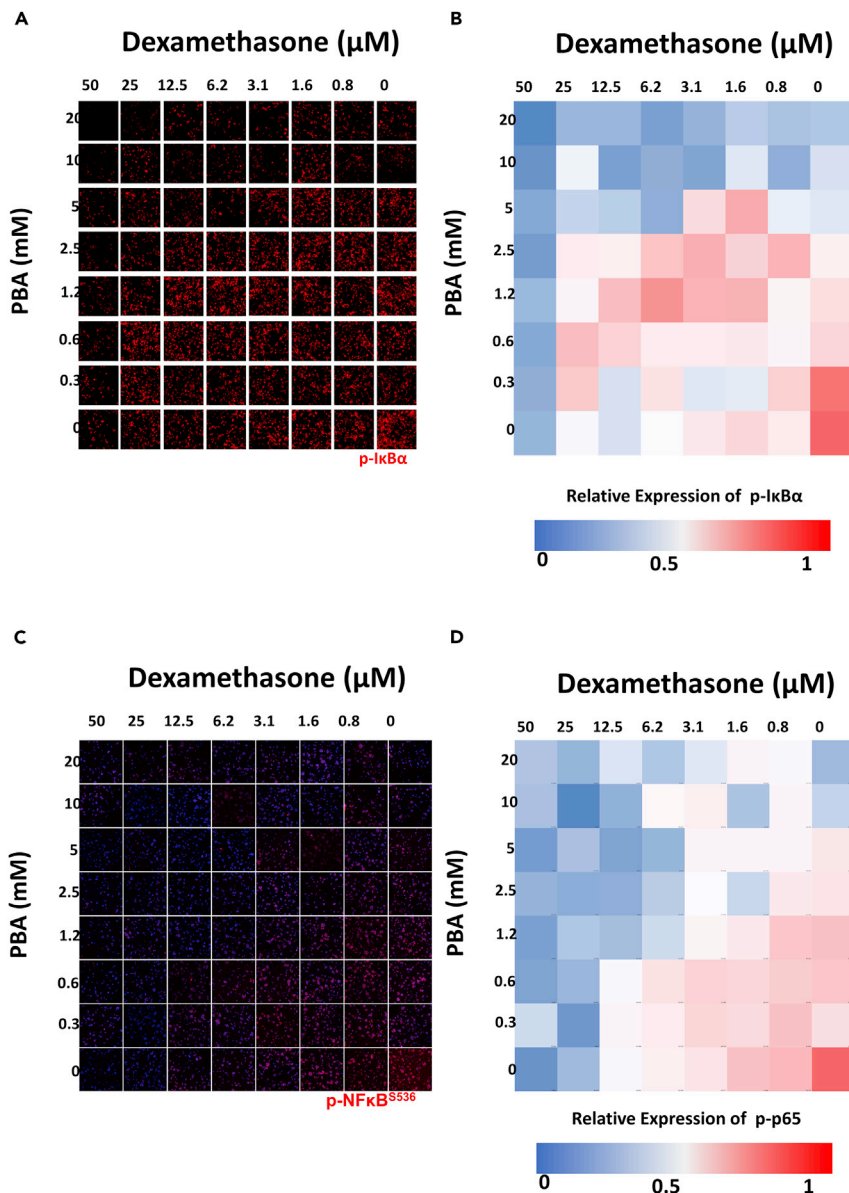


Figure 7. PBA synergizes with dexamethasone to reduce inflammation

(A) THP-1 cells were stimulated with LPS for 1 h followed by treatment with combinations of PBA and dexamethasone at varying concentrations. At 4 h post LPS stimulation, the cells were stained for p-I $\kappa\text{B}\alpha$ and processed for immunofluorescence microscopy. Levels of p65 for each drug combination were measured.

(B) Heatmap of relative expression of p-I $\kappa\text{B}\alpha$ from the immunofluorescence microscopy. Values were normalized to that of the LPS-stimulated, untreated control (bottom right image). Relative fold change for each drug combination as a ratio of (p-I $\kappa\text{B}\alpha$ level of the combination/p-I $\kappa\text{B}\alpha$ level of the untreated control) is provided. A corresponding checkerboard and heatmap are provided to measure p-p65 levels after 1 h of LPS stimulation in THP-1 cells (C and D).

dexamethasone are initially contraindicated for dendritic keratitis as they are immunosuppressive and may worsen symptoms of disease.³⁷ Reactivation of the virus has been observed in *in vitro* models of disease,¹⁷ and case series have implicated corticosteroids as a trigger for HSV epithelial keratitis.^{38,39} Thus, current guidelines recommend both antiviral and corticosteroid therapy in concert for treating HSV stromal keratitis.³⁷ PBA has been shown to act as an antiviral against HSV in both ocular and genital models of infection.⁴⁰ Therefore, since PBA has both antiviral and anti-inflammatory properties, it could be used alone as an alternative to combination therapy which may increase adherence and lower the risk of side effects.

Additionally, our study provides exciting evidence that PBA can synergize with existing corticosteroids such as dexamethasone to reduce inflammation. Dexamethasone has been shown to synergize with drugs such as lenalidomide, ruxolitinib, selinexor, and dasatinib for the treatment of certain cancers.^{41–44} However, dexamethasone has not been shown to synergize with FDA-approved medications for the alleviation of inflammation. Recently, it has been shown that fumaric acid esters can synergize with dexamethasone to inhibit NF- κ B signaling.⁴⁵ Here, we show that PBA may compose an alternative therapy which synergizes with DEX. Dexamethasone is used to treat a variety of inflammatory diseases such as ulcerative colitis, arthritis, lupus, and certain allergic disorders.^{39,46–48} Common side effects of DEX include swelling of the extremities, blurred vision, headache, depression, and weight gain.^{39,46,48} Reducing the required dosage of DEX while maintaining efficacy through PBA-DEX combination therapy may decrease the likelihood of these side effects occurring in patients.

While the PBA gel did not demonstrate increased antiviral activity, it did significantly reduce the inflammation observed in murine eyes post infection. It is important to develop sodium-free methods of PBA delivery as NaPBA adds to the sodium burden of patients and has decreased absorption compared to free PBA due to its decreased lipophilicity. Therefore, pairing PBA with P407 constitutes a more clinically viable alternative to improve mucosal penetration and delivery of the drug.

While PBA demonstrated reductions in cytokine release at the protein level following LPS and TG treatment (Figures 2 and 4), it was less efficacious in reducing cytokine production by poly(I:C) (Figure 3). There are a few reasons why we did not see the expected decrease in cytokine protein levels. Each inflammatory stimulus has a different time course of stimulating cytokine production and release. It may be the case that using an earlier or later time point would have been better to capture cytokine release with poly(I:C). While TNF- α increased dramatically by 24 h and decreased with PBA treatment, other cytokines might be stimulated at different times. Additionally, the levels of IL-6 and especially IL-8 were slightly decreased with PBA treatment. Furthermore, the effective concentration of PBA may have declined considerably by 24 h, and another bolus of PBA may have caused the cytokine production to fall. Another limitation of using the Multiplex ELISA was the limited sample size per treatment condition ($n = 2$). Using a greater number of samples may provide the statistical power needed to capture differences in these inflammatory cytokines.

In this study, we observed significant decreases in the phosphorylation of p-I κ B α and p-p65 with PBA treatment after stimulation with LPS or poly(I:C). Interestingly, total I κ B α declines with PBA treatment as well which would traditionally indicate that p65 is free to translocate to the nucleus and promote the transcription of pro-inflammatory cytokines. We believe that this discrepancy is due to the time points examined and the differences in I κ B α transcripts after LPS, poly(I:C), and PBA treatment. When performing initial experiments in our model set, we found that p-I κ B α gradually increases after LPS or poly(I:C) stimulation and peak at 4 h post treatment. Additionally, LPS and poly(I:C) stimulate I κ B α transcription as well (Figures 3 and 4). As PBA reduces I κ B α transcription, there may be less translated and subsequently phosphorylated with PBA treatment which would account for the decreases in both p-I κ B α and I κ B α seen in Figure 6A. While the differences in p-I κ B α may be due in part to the decrease in I κ B α transcription, our other data show that PBA acts as an anti-inflammatory agent at earlier time points. In the immunofluorescence images, we observe nuclear translocation of p65 at 15 min with 1 μ g/mL LPS treatment. However, p65 is precluded from the nucleus if PBA is added with LPS. Furthermore, we show in Figure S7 that I κ B α is degraded with 1 μ g/mL LPS treatment at 30 min, and this degradation is impeded by PBA. Coupled with the decreases in p-p65 observed with PBA treatment (Figure 6B), we conclude that PBA still antagonizes the NF- κ B pathway to restrict inflammatory signaling.

In conclusion, this study highlights how PBA can be used to relieve inflammation caused by ER stress, bacterial endotoxins, and viral genome mimetics *in vitro*. PBA inhibits the phosphorylation of I κ B α which prevents the downstream translocation of NF- κ B to the nucleus. PBA also inhibits phosphorylation of p65 which enhances NF- κ B transcriptional activity. PBA can be used *in vivo* to treat herpetic keratitis and reduce corneal thickness and ulceration. Additionally, PBA can synergize with DEX to impede NF- κ B signaling and subsequent inflammation. While PBA is well known as an ammonia scavenger and a chemical chaperone to treat urea cycle disorders and ER stress, respectively, PBA can also act as an anti-inflammatory therapy both alone and in conjunction with dexamethasone. Further studies should determine translational uses for PBA in disarming the inflammatory response and examine if its synergy with DEX can be translated into better clinical outcomes as well.

Limitations of the study

The limitations of this study include the discrepant experimental timelines which hinder the interpretation of PBA's effect on the NF- κ B pathway. While we observed prevention of nuclear translocation of NF- κ B and I κ B α degradation in 15 and 30 min, the reduction in total and p-I κ B α is seen in western blots only at 4 h. Reduction in p-p65 is also observed at these timepoints, while total levels of p65 were only observed using immunofluorescence microscopy. Nonetheless, the datasets argue an overall reduction in NF- κ B activity upon PBA treatment. Another limitation of this study includes the use of only two replicates for Multiplex ELISA experiments which does not allow for statistical analysis to be performed. However, our Multiplex ELISA results show a trend in concordance with our mRNA transcript datasets for inflammatory cytokines.

STAR★METHODS

Detailed methods are provided in the online version of this paper and include the following:

- KEY RESOURCES TABLE
- RESOURCE AVAILABILITY
 - Lead contact
 - Materials availability
 - Data and code availability
- EXPERIMENTAL MODEL AND SUBJECT DETAILS
 - Cell lines
 - Viruses
 - *In vivo* mouse studies
 - Chemical reagents
- METHOD DETAILS
 - Preparation of hypotonic gelling solution containing sodium salt of 4-phenylbutyric acid (Na-PBA)
 - *In vivo* HSV-1 infection
 - Real-time qPCR
 - Multiplex ELISA assay
 - Western blot
 - Immunofluorescence microscopy
 - *In vivo* herpetic keratitis model and treatment
 - Immunohistochemistry
- QUANTIFICATION AND STATISTICAL ANALYSIS

SUPPLEMENTAL INFORMATION

Supplemental information can be found online at <https://doi.org/10.1016/j.isci.2022.105682>.

ACKNOWLEDGMENTS

This research was supported by the NIH grants: R24EY033598 (to D.S.). This content is solely the responsibility of the authors and does not necessarily represent the official views of the NIH.

AUTHOR CONTRIBUTIONS

Conceptualization, R.K., T.Y., D.S.; Methodology, R.K., T.Y., Y.S., S.M., A.D., D.S.; Validation, R.K., T.Y., Y.S., S.M., A.D., D.S.; Formal Analysis, R.K., T.Y., D.S.; Investigation, R.K., T.Y., Y.S., S.M., A.D., D.S.; Writing – Original Draft, R.K., T.Y., D.S.; Writing – Review & Editing, R.K., T.Y., Y.S., S.M., A.D., D.S.; Funding Acquisition, T.Y., A.D., D.S.; Resources, R.K., T.Y., Y.S., S.M., A.D., D.S.; Supervision, T.Y., A.D., D.S.

DECLARATION OF INTERESTS

The authors declare no competing interests.

Received: March 28, 2022

Revised: August 18, 2022

Accepted: November 23, 2022

Published: December 22, 2022

REFERENCES

- Liu, B., Chan, C.C., and Nussenblatt, R.B. (2012). Application of small molecules/macromolecules in ocular inflammatory diseases. *Antiinflamm. Antiallergy. Agents Med. Chem.* *11*, 113–120.
- Lobo, A.M., Agelidis, A.M., and Shukla, D. (2019). Pathogenesis of herpes simplex keratitis: the host cell response and ocular surface sequelae to infection and inflammation. *Ocul. Surf.* *17*, 40–49.
- Kersey, J.P., McMullan, T.F.W., and Broadway, D.C. (2005). Pupil block glaucoma after neodymium:YAG capsulotomy in a patient with a partially subluxated posterior chamber intraocular lens. *J. Cataract Refract. Surg.* *31*, 1452–1453.
- De Las Heras, J., Aldámiz-Echevarría, L., Martínez-Chantar, M.L., and Delgado, T.C. (2017). An update on the use of benzoate, phenylacetate and phenylbutyrate ammonia scavengers for interrogating and modifying liver nitrogen metabolism and its implications in urea cycle disorders and liver disease. *Expet Opin. Drug Metabol. Toxicol.* *13*, 439–448.
- Yam, G.H.F., Gaplovska-Kysela, K., Zuber, C., and Roth, J. (2007). Sodium 4-phenylbutyrate acts as a chemical chaperone on misfolded myocilin to rescue cells from endoplasmic reticulum stress and apoptosis. *Invest. Ophthalmol. Vis. Sci.* *48*, 1683–1690.
- Reilmann, Y., Gronau, I., Hansen, U., and Dreier, R. (2019). 4-Phenylbutyric acid reduces endoplasmic reticulum stress in chondrocytes that is caused by loss of the protein disulfide isomerase ERp57. *Oxid. Med. Cell. Longev.* *2019*, 6404035.
- Kusaczuk, M., Bartoszewicz, M., and Cechowska-Pasko, M. (2015). Phenylbutyric Acid: simple structure - multiple effects. *Curr. Pharmaceut. Des.* *21*, 2147–2166.
- Kusaczuk, M., Krętowski, R., Bartoszewicz, M., and Cechowska-Pasko, M. (2016). Phenylbutyrate—a pan-HDAC inhibitor—suppresses proliferation of glioblastoma LN-229 cell line. *Tumour Biol.* *37*, 931–942.
- Zeng, M., Sang, W., Chen, S., Chen, R., Zhang, H., Xue, F., Li, Z., Liu, Y., Gong, Y., Zhang, H., and Kong, X. (2017). 4-PBA inhibits LPS-induced inflammation through regulating ER stress and autophagy in acute lung injury models. *Toxicol. Lett.* *271*, 26–37.
- He, M., Huang, X.F., Gao, G., Zhou, T., Li, W., Hu, J., Chen, J., Li, J., and Sun, T. (2019). Olanzapine-induced endoplasmic reticulum stress and inflammation in the hypothalamus were inhibited by an ER stress inhibitor 4-phenylbutyrate. *Psychoneuroendocrinology* *104*, 286–299.
- Montane, J., de Pablo, S., Castaño, C., Rodríguez-Comas, J., Cadavez, L., Obach, M., Visa, M., Alcarraz-Vizán, G., Sanchez-Martinez, M., Nonell-Canals, A., et al. (2017). Amyloid-induced β -cell dysfunction and islet inflammation are ameliorated by 4-phenylbutyrate (PBA) treatment. *Faseb. J.* *31*, 5296–5306.
- Chen, X., Wang, Y., Xie, X., Chen, H., Zhu, Q., Ge, Z., Wei, H., Deng, J., Xia, Z., and Lian, Q. (2018). Heme oxygenase-1 reduces sepsis-induced endoplasmic reticulum stress and acute lung injury. *Mediat. Inflamm.* *9413876*
- Valentine, M.S., Link, P.A., Herbert, J.A., Kamga Gninzeko, F.J., Schneck, M.B., Shankar, K., Nkwocha, J., Reynolds, A.M., and Heise, R.L. (2018). Inflammation and monocyte recruitment due to aging and mechanical stretch in alveolar epithelium are inhibited by the molecular chaperone 4-phenylbutyrate. *Cell. Mol. Bioeng.* *11*, 495–508.
- Zode, G.S., Sharma, A.B., Lin, X., Searby, C.C., Bugge, K., Kim, G.H., Clark, A.F., and Sheffield, V.C. (2014). Ocular-specific ER stress reduction rescues glaucoma in murine glucocorticoid-induced glaucoma. *J. Clin. Invest.* *124*, 1956–1965.
- Maddineni, P., Kasetti, R.B., Kodati, B., Yacoub, S., and Zode, G.S. (2021). Sodium 4-phenylbutyrate reduces ocular hypertension by degrading extracellular matrix deposition via activation of MMP9. *Int. J. Mol. Sci.* *22*, 10095.
- Zode, G.S., Bugge, K.E., Mohan, K., Grozdanic, S.D., Peters, J.C., Koehn, D.R., Anderson, M.G., Kardou, R.H., Stone, E.M., and Sheffield, V.C. (2012). Topical ocular sodium 4-phenylbutyrate rescues glaucoma in a myocilin mouse model of primary open-angle glaucoma. *Invest. Ophthalmol. Vis. Sci.* *53*, 1557–1565.
- Du, T., Zhou, G., and Roizman, B. (2012). Induction of apoptosis accelerates reactivation of latent HSV-1 in ganglionic organ cultures and replication in cell cultures. *Proc. Natl. Acad. Sci. USA* *109*, 14616–14621.
- Wang, W., Ye, F., and Zhou, J.-. (2009). Advances of poloxamer 407 in situ gel used as drug carrier. *Chin. J. New Drugs* *18*, 699–704.
- Khan, S., Warade, S., and Singhavi, D.J. (2018). Improvement in ocular bioavailability and prolonged delivery of tobramycin sulfate following topical ophthalmic administration of drug-loaded mucoadhesive microparticles incorporated in thermosensitive in situ gel. *J. Ocul. Pharmacol. Therapeut.* *34*, 287–297.
- Abou-Shamat, M.A., Calvo-Castro, J., Stair, J.L., and Cook, M.T. (2019). Modifying the properties of thermogelling poloxamer 407 solutions through covalent modification and the use of polymer additives. *Macromol. Chem. Phys.* *220*, 1900173.
- Russo, E., and Villa, C. (2019). Poloxamer hydrogels for biomedical applications. *Pharmaceutics* *11*, 671.
- Popov, A. (2020). Mucus-penetrating particles and the role of ocular mucus as a barrier to micro- and nanosuspensions. *J. Ocul. Pharmacol. Therapeut.* *36*, 366–375.
- Zierden, H.C., Josyula, A., Shapiro, R.L., Hsueh, H.T., Hanes, J., and Ensign, L.M. (2021). Avoiding a sticky situation: bypassing the mucus barrier for improved local drug delivery. *Trends Mol. Med.* *27*, 436–450.
- <https://www.webmd.com/drugs/2/drug-176506/inveltys-ophthalmic-eye/details>.
- <https://www.drugs.com/newdrugs/fda-approves-eyvisis-loteprednol-etabonate-ophthalmic-suspension-short-term-signs-dry-eye-5375.html>.
- Schopf, L., Enlow, E., Popov, A., Bourassa, J., and Chen, H. (2014). Ocular pharmacokinetics of a novel loteprednol etabonate 0.4% ophthalmic formulation. *Ophthalmol. Ther.* *3*, 63–72.
- Schopf, L.R., Popov, A.M., Enlow, E.M., Bourassa, J.L., Ong, W.Z., Nowak, P., and Chen, H. (2015). Topical ocular drug delivery to the back of the eye by mucus-penetrating particles. *Transl. Vis. Sci. Technol.* *4*, 11.
- Kim, T., Sall, K., Holland, E.J., Brazzell, R.K., Coultas, S., and Gupta, P.K. (2019). Safety and efficacy of twice daily administration of KPI-121 1% for ocular inflammation and pain following cataract surgery. *Clin. Ophthalmol.* *13*, 69–86.
- Schaefer, L., Hernandez, H., Coats, R.A., Yu, Z., Pflugfelder, S.C., Britton, R.A., and de Paiva, C.S. (2022). Gut-derived butyrate suppresses ocular surface inflammation. *Sci. Rep.* *12*, 6581.
- Vane, J.R., and Botting, R.M. (1998). Anti-inflammatory drugs and their mechanism of action. *Inflamm. Res.* *47*, 78–87.
- Chen, L., Deng, H., Cui, H., Fang, J., Zuo, Z., Deng, J., Li, Y., Wang, X., and Zhao, L. (2018). Inflammatory responses and inflammation-associated diseases in organs. *Oncotarget* *9*, 7204–7218.
- Sharif, O., Bolshakov, V.N., Raines, S., Newham, P., and Perkins, N.D. (2007). Transcriptional profiling of the LPS induced NF- κ B response in macrophages. *BMC Immunol.* *8*, 1.
- Giridharan, S., and Srinivasan, M. (2018). Mechanisms of NF- κ B p65 and strategies for therapeutic manipulation. *J. Inflamm. Res.* *11*, 407–419.
- Furman, D., Campisi, J., Verdin, E., Carrera-Bastos, P., Targ, S., Franceschi, C., Ferrucci, L., Gilroy, D.W., Fasano, A., Miller, G.W., et al. (2019). Chronic inflammation in the etiology of disease across the life span. *Nat. Med.* *25*, 1822–1832.
- Dequeker, J. (1999). NSAIDs/corticosteroids—primum non nocere. *Adv. Exp. Med. Biol.* *455*, 319–325.
- https://www.accessdata.fda.gov/drugsatfda_docs.
- <https://www.aao.org/clinical-statement/herpes-simplex-virus-keratitis-treatment-guideline>.

38. Takeshita, T. (1996). Bilateral herpes simplex virus keratitis in a patient with pemphigus vulgaris. *Clin. Exp. Dermatol.* 21, 291–292.
39. el-Antably, S.A., and Atia, H.E. (1976). Ocular complications of corticosteroids. *Bull. Ophthalmol. Soc. Egypt* 69, 635–641.
40. Yadavalli, T., Suryawanshi, R., Koganti, R., Hopkins, J., Ames, J., Koujah, L., Iqbal, A., Madavaraju, K., Agelidis, A., and Shukla, D. (2020). Standalone or combinatorial phenylbutyrate therapy shows excellent antiviral activity and mimics CREB3 silencing. *Sci. Adv.* 6, eabd9443.
41. Ma, J., Wu, K., Bai, W., Cui, X., Chen, Y., Xie, Y., and Xie, Y. (2017). Synergistic cytotoxicity of lenalidomide and dexamethasone in mantle cell lymphoma via cereblon-dependent targeting of the IL-6/STAT3/PI3K Axis. *EBioMedicine* 20, 70–78.
42. Verbeke, D., Gielen, O., Jacobs, K., Boeckx, N., De Keersmaecker, K., Maertens, J., Uyttebroeck, A., Segers, H., and Cools, J. (2019). Ruxolitinib synergizes with dexamethasone for the treatment of T-cell acute lymphoblastic leukemia. *HemaSphere* 3, e310.
43. Chen, C.I., Gutierrez, M., Siegel, D.S., Richter, J.R., Wagner-Johnston, N., Hofmeister, C.C., Berdeja, J.G., Gabrail, N., Baz, R., Mau-Sorensen, M., et al. (2014). Selinexor demonstrates marked synergy with dexamethasone (Sel-Dex) in preclinical models and in patients with heavily pretreated refractory multiple myeloma (MM). *Blood* 124, 4773.
44. Shi, Y., Beckett, M.C., Blair, H.J., Tirtakusuma, R., Nakjang, S., Enshaei, A., Halsey, C., Vormoor, J., Heidenreich, O., Krippner-Heidenreich, A., and van Delft, F.W. (2021). Phase II-like murine trial identifies synergy between dexamethasone and dasatinib in T-cell acute lymphoblastic leukemia. *Haematologica* 106, 1056–1066.
45. Genito, C.J., Eckshtain-Levi, M., Piedra-Quintero, Z.L., Krovi, S.A., Kroboth, A., Stiepel, R.T., Guerau-de-Arellano, M., Bachelder, E.M., and Ainslie, K.M. (2021). Dexamethasone and fumaric acid ester conjugate synergistically inhibits inflammation and NF- κ B in macrophages. *Bioconjugate Chem.* 32, 1629–1640.
46. <https://pubchem.ncbi.nlm.nih.gov/compound/5743>.
47. Williams, H.P., Falcon, M.G., and Jones, B.R. (1977). Corticosteroids in the management of herpetic eye disease. *Trans. Ophthalmol. Soc. U. K.* 97, 341–344.
48. Ramamoorthy, S., and Cidlowski, J.A. (2016). Corticosteroids-mechanisms of action in health and disease. *Rheum. Dis. Clin. North Am.* 42, 15–31.
49. Lund, M.E., To, J., O'Brien, B.A., and Donnelly, S. (2016). The choice of phorbol 12-myristate 13-acetate differentiation protocol influences the response of THP-1 macrophages to a pro-inflammatory stimulus. *J. Immunol. Methods* 430, 64–70.
50. Ames, J., Yadavalli, T., Suryawanshi, R., Hopkins, J., Agelidis, A., Patil, C., Fredericks, B., Tseng, H., Valyi-Nagy, T., and Shukla, D. (2021). OPTN is a host intrinsic restriction factor against neuroinvasive HSV-1 infection. *Nat. Commun.* 12, 5401–5414.

STAR★METHODS

KEY RESOURCES TABLE

REAGENT or RESOURCE	SOURCE	IDENTIFIER
Antibodies		
p-IκBa	Cell Signaling Technology (CST)	Cat#2859
IκBa	CST	Cat#4814
p-p65	CST	Cat#3031
p65	CST	Cat#3033
GAPDH	ProteinTech	Cat#10494-1-AP; RRID:AB_2263076
Secondary Alexa Fluor 647 Antibody	Invitrogen	Cat#A21246
Horse radish Peroxidase-Conjugated IgG antibodies	Jackson ImmunoResearch Laboratories	615-035-214; 611-035-215
Bacterial and virus strains		
HSV-1 McKrae	Dr. Patricia Spear	N/A
Chemicals, Peptides, and Recombinant proteins		
Sodium salt of 4-PBA	Cayman Chemical Company (MI, USA)	1716-12-7
Kolliphor® P 407	BASF (NJ, USA)	N/A
Sodium-free PBA	BioVision	Cat#1608-1000
Thapsigargin	Selleck Chemicals (TX, USA)	Cat#S7895
Acyclovir (ACV)	Selleck Chemicals	Cat#S1807
Lipopolysaccharide	Sigma-Aldrich	Cat#L2630
poly(I:C)	Sigma-Aldrich	Cat#P1530
Dexamethasone	Selleck Chemicals	Cat#S3124
Lipofectamine RNAiMAX Transfection Reagent	ThermoFisher Scientific	Cat#13778075
Phorbol 12-myristate 13-acetate (PMA)	Sigma-Aldrich	Cat#P8139
TRIzol	Life Technologies	Cat#15596-026
High-Capacity cDNA Reverse Transcription Kit	Applied Biosystems (Foster City, CA)	Cat#4368814
Fast SYBR Green Master Mix	ThermoFisher Scientific	Cat#4385612
Experimental models: Cell lines		
Human corneal epithelial (HCE) cells	Kozaburo Hayashi	Cat#RCB1384 HCE-T; RRID:CVCL_1272
THP-1 cells	Dr. Afsar Naqvi	N/A
Experimental models: Organisms/Strains		
C57BL/6 mice	Charles River Laboratories	N/A
Oligonucleotides		
Primers	See manuscript for a list of oligonucleotides	Integrated DNA Technologies
Software and algorithms		
GraphPad Prism	Dotmatics	(version 4.0)

RESOURCE AVAILABILITY

Lead contact

Further information and requests for resources and reagents should be directed to and will be fulfilled by the lead contact, Deepak Shukla (dshukla@uic.edu).

Materials availability

All reagents were purchased commercially. This study did not generate new unique reagents.

Data and code availability

- Original Western blot images have been listed as supplementary figures in the supplementary materials file. All data reported in this paper will be shared by the [lead contact](#) upon request.
- This paper does not report original code.
- Any additional information required to reanalyze the data reported in this paper is available from the [lead contact](#) upon request.

EXPERIMENTAL MODEL AND SUBJECT DETAILS

Cell lines

HCE cells (RCB1834 female HCE-T) were provided by Kozaburo Hayashi. HCE cells were cultured in minimum essential medium (MEM; Life Technologies, Carlsbad, CA) with 10% fetal bovine serum (FBS; Sigma-Aldrich, St. Louis, MO) and 1% penicillin-streptomycin (P/S; Life Technologies) at 37°C and 5% CO₂. The human monocytic THP-1 cell line was a gift from Dr. Afsar Naqvi (University of Illinois at Chicago). THP-1 cells were cultured in RPMI media (Life Technologies) with 10% FBS and 1% P/S at 37°C and 5% CO₂. THP-1 cells were stimulated with 25 nM phorbol 12-myristate 13-acetate (PMA; Sigma-Aldrich) for 72 h before changing the media to PMA-free RPMI for 24 h.⁴⁹ After the recovery period, they were used for experiments. All cell lines have been validated in a previous manuscript.⁵⁰

Viruses

The HSV-1 McKrae strain used for *in vivo* infection was provided by Dr. Patricia Spear (Northwestern University). Virus stocks were produced and titrated using Vero cells.

In vivo mouse studies

Procedures to care for the mice and maintenance of murine colonies were performed according to a protocol approved by the Animal Care Committee at the University of Illinois at Chicago. The mice were purchased from a university-approved vendor source: Charles River Laboratories. Animals were group housed, fed an *ad libitum* diet, and caged at room temperature. Eight-week-old male C57BL/6 mice were used for these experiments, and male littermates were randomly assigned to experimental groups.

Chemical reagents

Sodium salt of 4-phenylbutyric acid (Na-PBA) was purchased from Cayman Chemical Company (MI, USA) and dissolved in DMSO to make a 5 M stock solution that was further diluted to 5 mM or 20 mM for *in vitro* experiments. Kolliphor P 407 was obtained as a gift sample from BASF (NJ, USA). Sodium free PBA was purchased from BioVision (1608-1000) and used at 5 mM for HCE cells and 20 mM for THP-1 cells. TG (Selleck Chemicals, TX, USA) was used at 1-10 μM while ACV was used at 50 μM (Selleck Chemicals). LPS and poly(I:C) were both purchased from Sigma-Aldrich and used at 100 ng/mL and 25 μg/mL unless otherwise stated. Dexamethasone was purchased from Selleckchem and used at 0-50 μM. To induce an inflammatory response *in vitro*, TG, LPS, poly(I:C), or NaCl (50 mM) were given at the appropriate concentrations for 1 h. Poly(I:C) was added in opti-MEM (Life Technologies) with 1 μL/mL Lipofectamine RNAiMAX Transfection Reagent (Thermo Fisher Scientific). PBA or DMSO was then added afterward for 3 h. Cells were then collected for further processing.

METHOD DETAILS

Preparation of hypotonic gelling solution containing sodium salt of 4-phenylbutyric acid (Na-PBA)

The hypotonic gelling solution (Ref: <https://pubmed.ncbi.nlm.nih.gov/32895514/>) of Na-PBA was prepared in 10% (w/v) Kolliphor P407 solution using cold method. Briefly, 1 g of Kolliphor P 407 was added in a 20 mL scintillation vial containing 10 mL of distilled water. The vial containing dispersion was stored in a refrigerator at 4°C and vortexed periodically until the P407 dissolved completely. Further, Na-PBA (500 mg) was weighed and dissolved in the prepared 10% (w/v) Kolliphor P 407 solution to make 5% (w/v) Na-PBA hypotonic gelling solution. The concentration mentioned in the manuscript (10 mg/mL or ~61 mM) was the highest achievable loading concentration of PBA in P407. This formulation was stable at room temperature and did not precipitate over a period of 1 month. Hence, this concentration was used. The concentration is also

consistent with ophthalmic Trifluridine(1%W/V or 33 mM) ophthalmic drops or Acyclovir(3%W/W or 133 mM) gel prescribed clinically.

In vivo HSV-1 infection

On day 0, $n = 5$ mice were anesthetized with an intraperitoneal injection of ketamine (100 mg/kg) and xylazine (5 mg/kg). Afterward, they were given 0.5% proparacaine hydrochloride topically. Corneal epithelial debridement in a 3×3 grid pattern was performed using a 30-gauge needle. A total of 5×10^5 PFU HSV-1 McKrae viruses were overlaid on the debrided cornea in a total volume of 5 μ L. Animals were monitored until awake and then allowed to return to their cages. Murine corneas were treated with PBA-hypotonic gel with ganciclovir (0.1%) and PBS as positive and negative control respectively. Treatments were given as 5 μ L eye drops 3 times every day for 5 days. On day 2 and 4 post infection, ocular washes were collected in Opti-MEM for viral titration. Ocular washes were collected prior to first treatment dose of the day. Virus titration was performed on Vero Cells to quantify extent of infectious virus prevalent in murine eyes. Ocular HSV-1 disease scoring was performed by a blinded reviewer to determine extent of peri-ocular inflammation, blepharitis, and corneal scarring from 0 to 4 (4 being severe). Animal weights were monitored daily until the end of the experimental period. Any animals showing excessive scarring, inflammation, weight loss (>15%) and ataxia were euthanized according to ACC protocols. OCT images procured from the instrument were loaded into ImageJ software. Using the measure function, the total corneal thickness was evaluated. Images procured the day before the treatment began were normalized to 100% thickness. The thickness of the cornea for subsequent weeks was compared to the start-day thickness. As all animals were ear-tagged, each corneal thickness was compared to its own previous image to understand the percentage decrease in thickness over the course of 4 weeks.

Real-time qPCR

Cells were collected in TRIzol (Life Technologies), and the RNA was isolated as per the manufacturer's protocol. The RNA samples were dissolved in Molecular Biology Grade Water (Corning, USA) and quantified using NanoDrop (Thermo Fisher Scientific). 1 μ g of RNA from each sample was reverse transcribed into cDNA using the High-Capacity cDNA Reverse Transcription Kit (Applied Biosystems, Foster City, CA). Real-time quantitative PCR was performed using the cDNA and a Fast SYBR Green Master Mix on the QuantStudio 7 Flex system (Applied Biosystems). The following primers were used in this study from 5' to 3': GAPDH forward: CACCACCAACTGCTTAGCAC, GAPDH reverse: CCCTGTTGCTGTAGCCAAAT, TNF- α forward: AGCCCATGTTGTAGCAAACCC, TNF- α reverse: GGACCTGGGAGTAGATGAGGT, IL-1 β forward: TCGCCAGTGAAATGATGGCT, IL-1 β reverse: TGGGAAGGAGCACTTCATCTGTT, IL-6 forward: TGACAAACAAATTGGGTACATCCT, IL-6 reverse: AGTGCCTGTTGCTGCTTTCAC, IL-8 forward: GCGCCAACACAGAAATTATTGTAA, IL-8 reverse: TTATGAATTCTCAGCCCTCTCAA, MMP-9 forward: TGTACC GCTATGGTTACTACTCG, MMP-9 reverse: GGCAGGGACAGTTGCTTCT, I κ B α forward: TCCACTCCAT CCTGAAGGCTAC, I κ B α reverse: CAAGGACACCAAAAGCTCCACG, CCL5 forward: TGTACTCCCGA ACCCATTTT, CCL5 reverse: TACACCAGTGGCAAGTGCTC, CHOP forward: CATCACCACACCTGAA AGCAGA, CHOP reverse: TGGACAGTGTCCGGAAGGAG, IFN- α forward: GATGACAACCAGTTCCA GAAG, IFN- α reverse: AAAGAGGTTGAAGATCTGCTGGAT, IFN- β forward: CTCCACTACAGCTGTT TCCAT, IFN- β reverse: GTCAAAGTTCATCCTGTCCT.

Multiplex ELISA assay

Supernatants were removed from cells and centrifuged at 16,000 g. The clarified supernatant was transferred to a fresh tube and used for the Milliplex Human Cytokine/Chemokine/Growth Factor Panel A to measure cytokine levels. The following cytokines were measured in the panel: TNF- α , IL-1 β , IL-2, IL-4, IL-6, IL-8, IL-18, IFN- α , IFN- γ , and VEGF-A. Representative multiplex ELISA was performed using 2 samples in duplicate for each condition.

Western blot

HCE or THP-1 cells were collected in Hank's Balanced Salt Solution (Life Technologies) and pelleted by centrifugation at 800 g for 5 min. The pellets were dissolved in Radio Immunoprecipitation Assay (RIPA) buffer (Sigma-Aldrich) with Halt Protease Phosphatase Inhibitor Cocktail 100X (Thermo Fisher Scientific). Samples were incubated at 4°C for 30 min and spun down at 16,000 g for 20 min. The supernatants were transferred to a fresh set of tubes and mixed with NuPAGE LDS Sample Loading Buffer (Life Technologies) and 5% beta-mercaptoethanol (Thermo Fisher Scientific). The samples were then denatured at 90°C for

9 min. After gel electrophoresis was performed, the proteins were transferred onto a nitrocellulose membrane (IB23001; Invitrogen) via an iBlot 2 dry transfer machine. The membranes were blocked in 5% nonfat milk in tris-buffered saline (TBS; Thermo Fisher Scientific) and 0.1% Tween 20 (Sigma-Aldrich) (TBST) for 1 h at room temperature. 1:1,000 dilutions of primary antibodies in 5% milk were added after blocking and left to incubate on a shaker overnight at 4°C. The following day, the blots were washed three times with TBST at 5 min intervals. The appropriate secondary antibody (anti-rabbit or anti-mouse) was added onto the blots at a 1:5,000 dilution for 1 h at room temperature. After 3 more washes with TBST, Super-Signal West Pico maximum sensitivity substrate was added to the blots. Protein bands were visualized using an ImageQuant LAS 4000 imager (GE Healthcare Life Sciences), and their densities were quantified in ImageJ. The original unedited blots used in the paper are provided in [Figures S8–S11](#).

Immunofluorescence microscopy

Cells were plated and underwent experimentation in glass bottom dishes (MatTek Corporation). The cells were then washed with PBS and fixed using 4% paraformaldehyde (Electron Microscopy Sciences, Hatfield, PA) for 10 min. After another wash with PBS, they were permeabilized with 0.1% Triton X-100 (Thermo Fisher Scientific) for 10 min. The cells were washed and blocked in 0.1% BSA for 1 h at room temperature. They were then incubated with a primary antibody in 0.1% BSA for 1 h, washed using PBS, and left with a secondary conjugated Alexa Fluor 647 in 0.1% and one drop/mL of NucBlue Fixed Cell ReadyProbes Reagent for 1 h. The dishes were washed with PBS one final time and then imaged using an LSM 710 confocal microscope (Carl Zeiss). 63× images were taken for all experiments.

In vivo herpetic keratitis model and treatment

On day 0, $n = 50$ mice were anesthetized with an intraperitoneal injection of ketamine (100 mg/kg) and xylazine (5 mg/kg). Afterward, they were given 0.5% proparacaine hydrochloride topically. Corneal epithelial debridement in a 3×3 grid pattern was performed using a 30-gauge needle. 1×10^5 PFU/mL HSV-1 McKrae was applied immediately afterward to the ocular surface. Mice were untreated for 4 weeks following infection to develop herpetic keratitis. A subset of the mice ($n = 22$) developed keratitis, while the other mice ($n = 28$) either did not develop keratitis or had severe ulceration of the cornea. The mice with mild keratitis were divided into two groups ($n = 11$ each) and treated with 5 mM PBA or DMSO topically three times per day. OCT images were taken on an SPECTRALIS OCT module (Heidelberg Engineering) at 4 weeks post infection and weekly for another four weeks. OCT images procured from the instrument were loaded into ImageJ software. Using the measure function, the corneal thickness was evaluated. Images procured the day before the treatment began were normalized to 100% thickness. The thickness of the cornea for subsequent weeks was compared to the start-day thickness. As all animals were ear-tagged, each corneal thickness was compared to its own previous image to understand the percentage decrease in thickness over the course of 4 weeks.

Immunohistochemistry

At 8 weeks post infection and 4 weeks post treatment, the mice were euthanized, and whole eye tissue was collected and embedded in optimal cutting temperature (OCT) compound for sectioning. Embedded whole eye samples were sectioned using an NX50 Cryostat (Thermo Fisher Scientific). Sections were mounted onto slides, and the slides were fixed using ice-cold acetone for 5 min. Each slide underwent the following procedure for hematoxylin & eosin staining: 1) 2 min wash with de-ionized water, 2) 1 min hematoxylin stain, 3) 2 min water wash, 4) 2 min in 70% ethanol, 5) 2 min in 100% ethanol, 6) 1 min eosin stain, 7) 2 min in 70% ethanol, 8) 2 min in 100% ethanol, and 9) 2 min in xylene. The slides were dried, and coverslips were mounted using Permount Mounting Medium (Thermo Fisher Scientific). Slides were then imaged using an Axioskop 2 microscope (Carl Zeiss).

QUANTIFICATION AND STATISTICAL ANALYSIS

GraphPad Prism software (version 4.0) was used for statistical analysis between groups for the experiments in the paper. T-tests were used to compare continuous variables between two groups, and one-way ANOVAs were used to compare continuous variables between three groups. n represents the number of times an experiment was independently performed for *in vitro* studies and the number of animals/samples in each group for *in vivo* studies. Significance was defined based on exceeding different p value thresholds: * = $p < 0.05$, ** = $p < 0.01$, *** = $p < 0.001$, **** = $p < 0.0001$.